DOE/PC/94066--T8

Isobutanol-Methanol Mixtures from Synthesis Gas

Quarterly Technical Progress Report

Period Covered: 1 July to 30 September 1996

Contractor

University of California-Berkeley
Berkeley, California 94720

Enrique Iglesia - Program Manager

4 December 1996

Prepared for the United States Department of Energy *
Under Contract Number DE-AC22-94PC94066
Contract Period 1 October 1994 - 30 September 1997

DISCLAIMER

* This report was prepared as an account of work sponsored by the United States Government. Neither the United States Government nor the United States Department of Energy, nor any of their employees, make any warranty, express or implied, or assumes any legal liability or responsibility for the accuracy, completeness, or usefulness of any information, apparatus, product, or process disclosed, or represents that its use would not infringe privately owned rights. Reference herein to any specific commercial product, process, or service by trade name, trademark, manufacturer, or otherwise does not necessarily constitute or imply its endorsement, recommendation, or favoring by the United States Government or any agency thereof. The views and opinions of authors expressed herein do not necessarily state or reflect those of the United State Government or any agency thereof.

TABLE OF CONTENTS

EXECUTIVE SUMMARY

1. CONTRACT OBJECTIVES AND TASKS

2. SUMMARY OF ACTIVITIES

3. STATUS, ACCOMPLISHMENTS, AND RESULTS

Task 1: Project Work Plan

Task 2: Catalyst Synthesis

Task 3: Catalyst Evaluation in Laboratory Scale Reactors

3.1 Kinetic Studies of Alcohol Coupling Reactions

3.2 Isobutanol Synthesis at High Pressure in the CMRU

Task 4: Identification of Reaction Intermediates

4.1 Measurements of Copper Surface Area
4.2 Determination of Basic Site Density and Strength

Task 5: Bench-Scale Catalyst Evaluation at Air Products and Chemicals

4. PARTICIPATING PROJECT PERSONNEL

EXECUTIVE SUMMARY

A series of $CuMgCeO_x$ catalysts have been prepared by coprecipitating the corresponding metal nitrates with a mixed solution of potassium carbonate and potassium hydroxide. The bulk composition of the catalyst has been measured by atomic absorption (AA) analysis and the Cu dispersion has been determined by N_2O titration at 90 °C. CeO_x does not contribute to the measured copper dispersion in $K\text{-}Cu_{0.5}Mg_5CeO_x$ samples and the high dispersion value indeed reflects the presence of Cu metal small crystallites.

Kinetic studies of methanol and propionaldehyde coupling reactions on $K\text{-}Cu/MgO/CeO_2$ and MgO/CeO_2 catalysts indicate that Cu enhances the rates of alcohol dehydrogenation. The cross-coupling reactions of propionaldehyde and ^{13}C-labeled methanol produce singly-labeled isobutyraldehyde, a precursor to isobutanol, suggesting that it forms by the condensation of propionaldehyde and a reactive intermediate derived from methanol. Singly-labeled propionaldehyde formed by the reverse aldol condensation of 2-methyl-3-hydroxy-propionaldehyde. The latter formed by the cross coupling between propionaldehyde and ^{13}C-labeled methanol followed by hydrogen transfer from γ–carbon atom and hydroxyl group to the carbonyl group. Methanol reactions on MgO form only CO and CO_2 with trace amounts of methyl formate. The addition of AlO_x to MgO leads to the formation of dimethylether (DME), suggesting the presence of acid sites resulting from the separate phases of AlO_x. DME-to-CO_x ratio increases with increasing Al content.

High-pressure isobutanol synthesis from CO/H_2 has been studied on $Cu_{0.5}Mg_5O_x$ catalysts at 593 K and 4.5 MPa. $Cu_{0.5}Mg_5O_x$ catalysts show high hydrocarbon and low isobutanol selectivities compared to $K\text{-}Cu_{0.5}Mg_5CeO_x$, suggesting the presence of residual acidity in $Cu_{0.5}Mg_5O_x$. Methanol turnover rates on $Cu_{0.5}Mg_5O_x$ are higher than on $K\text{-}Cu_{0.5}Mg_5CeO_x$, suggesting that the active site (Cu) for methanol synthesis is inhibited by reaction products such as CO_2 and H_2O. The small Cu crystallites resulting from the interaction between copper and cerium oxides are more likely to be oxidized by CO_2 and/or H_2O.

The density and strength of available basic sites are determined using a $^{13}CO_2/^{12}CO_2$ isotopic exchange method. Addition of CeO_x to MgO increases not only MgO surface area but also the density and strength of available basic sites at 573 K. The presence of Cu has little effect on basic site density and strength in $Cu_{0.5}Mg_5CeO_x$. Yet, K increases both the density and strength of basic sites. Mg_5AlO_x mixed-oxides exhibit lower basic site density and strength compared to MgO.

Two manuscripts *"Isobutanol and Methanol Synthesis on Copper Catalysts Supported on Modified Magnesium Oxide"* and *"Isotopic Switch Methods for the Characterization of Basic Sites in Modified MgO Catalysts"* are in the final draft and will be submitted for publication during the next reporting period.

1. CONTRACT OBJECTIVES AND TASKS

The contract objectives are:

1. To design a catalytic material for the synthesis of isobutanol with a productivity of 200 g isoalcohols/g-cat-h and a molar isobutanol-to-methanol ratio near unity

2. To develop structure-function rules for the design of catalysts for the selective conversion of synthesis gas to isoalcohols

The research program has been grouped into five specific tasks and a set of project management and reporting activities. The abbreviated designations for these tasks are:

- Project Work Plan ***(Task 1)***

- Catalyst Synthesis ***(Task 2)***

- Catalyst Evaluation in Laboratory Scale Reactors ***(Task 3)***

- Identification of Reaction Intermediates ***(Task 4)***

- Bench-Scale Catalyst Evaluation at Air Products and Chemicals ***(Task 5)***

2. SUMMARY OF ACTIVITIES

Activities during this period have focused on:

- Preparation of a series of K-Cu/MgO/CeO_2, CuCoMgCeO_x, and MgAlOx catalysts

- Measurements of Copper Surface Area

- Determination of basic site density and strength at reaction temperatures using $^{13}CO_2/^{12}CO_2$ switch methods

- Isotopic tracer studies of alcohol coupling reactions on MgO/CeO_2 and MgO/Al_2O_3-based catalysts

- Evaluation of high-pressure isobutanol synthesis reactions on $Cu_{0.5}Mg_5O_x$ catalysts

3. STATUS, ACCOMPLISHMENTS, AND RESULTS

Task 1: Management Plan

No activities were carried out during this reporting period.

Task 2: Catalyst synthesis

$CuCeMgO_x$ and its individual components were prepared by coprecipitation of 1 M mixed metal nitrate solutions with a mixed solution of potassium hydroxide (2 M) and potassium carbonate (1 M) at 338 K and a constant pH of 9 in a computer-controlled well-stirred batch reactor. The precipitates were filtered, washed with de-ionized water at 338 K, and then dried at 353-363 K overnight. The resulting materials were calcined at 723 K for 4 h to obtain the mixed oxides. The detailed procedures have been described by Apesteguia et al. [1]. K-containing samples were prepared by incipient wetness impregnation using K_2CO_3 (0.25 M) solutions. The nominal potassium concentration was 1.0 wt.%. Catalyst properties are summarized in Table 1.

Table 1. Composition and surface areas of metal oxides.

Sample	**Nominal composition**	**Mg/Cu**	**Mg/Ce**	**K** (wt.%) AAS	**S.A.** (m^2 / g)
MG 3 - 5 O/K	$Cu_{0.1}MgO_x$	8	---	1.1	112
MG 3 - 7 O/K	Mg_5CeO_x	---	5.2	0.7	155
MG 3 - 8 O/K	MgO	---	---	---	129
MG 3 - 9 O	CeO_2	---	---	< 0.01	80
MG 3 - 12 O	Mg_5CeO_x	---	4.8	0.01	183
MG 3 - 13 O	$Cu_{0.5}Mg_5CeO_x$	8.3	4.3	< 0.01	160

As mentioned in the previous report (3Q, FY'96), the amount of residual potassium on MG3-3 O (CeO_2), left behind during co-precipitation, was very high, resulting in a material with low surface area (S.A.=0.2 m^2/g). Another CeO_2 sample (MG3-9 O) was prepared by co-precipitation methods. The precipitates were filtered and ***thoroughly washed*** with distilled water at 338 K, resulting in a cerium oxide with low potassium content and high surface area (Table 1). New batches of Mg_5CeO_x (MG3-12 O) and $Cu_{0.5}Mg_5CeO_x$ (MG3-13 O) were synthesized in order to verify the reproducibility in catalyst preparation and to provide large amounts of sample for testing in CMRU.

At this point, we decided to prepare several new catalytic materials in order to 1) avoid CO_2 inhibition on Cu (by removing CeO_x to avoid Cu-Ce interaction) and on basic sites (by varing basic strength), 2) increase surface area (by Zr, Zn, and Mn addition) and basic site density and strength (by Li addition) of basic oxides, and 3) improve the chain growth by incorporating a chain growth component (Co) into the best $CuMgMeO_x$ material (Me=Ce, Al). Some of these materials have been prepared in collaboration with Professor Carlos Apesteguia's research group in the Department of Chemical Enginering

at Universidad Nacional del Litoral in Santa Fe (Argentina). A list of the materials being synthesized is given in Table 2.

Table 2. Catalysts being synthesized.

Catalyst	Synthesis Method
$CuZnAlO_x$	Coprecipitation
$CuZnAlO_x$/(K)$MgCeO_x$	Coprecipitation and Physical Mixtures
$CuZnAlO_x$/(K)$MgAlO_x$	Coprecipitation and Physical Mixtures
$CuZnAlO_x$/(K)MgOx	Coprecipitation and Physical Mixtures
$CuCoMgCeO_x$	Coprecipitation
$CuMgAlO_x$	Coprecipitation
$CuCoMgAlO_x$	Coprecipitation
$MgAlO_x$	Coprecipitation

$Cu_{0.5}Mg_5Al_{10}O_x$ (MG3-15 P), $Cu_{0.5}Co_{0.1}Mg_5Al_{10}O_x$ (MG3-16 P), and $MgAlO_x$ samples were provided by Apesteguia's research group. These samples were prepared by co-precipitation of 1.5 M mixed metal nitrate solutions with a mixture of KOH (2M) and K_2CO_3 (1M) at 333 K and a constant pH of 10 in a stirred-batch reactor following the procedures described by Apesteguia et al. [1]. The precipitates were filtered, washed with 600 ml of distilled water at 333 K and dried at 348 K overnight. Then, the precursors were crushed and suspended in 300 cm^3 of hot water, washed again with 600 cm^3 of hot water, filtered and dried at 348 K. The resulting precursors will be calcined at 723 K for 4 h to obtain the mixed oxides. The amount of residual potassium, determined by atomic analysis, was less than 0.05 wt.%.

Task 3: Catalyst Evaluation in Laboratory Scale Reactors

3.1 Kinetic Studies of Alcohol Coupling Reactions

Alcohol coupling reactions require a sequence of steps leading to the formation of higher alcohols from C_1 and C_2 alcohols [2,3]. These steps include alcohol dehydrogenation to aldehydes, aldol condensation of aldehydes to higher aldehydes and ketones, and the subsequent hydrogenation to higher alcohols. It is believed that aldehydes are the reactive intermediates in chain-growth reactions that occur on basic sites [4,5].

Ethanol dehydrogenation-coupling reactions were reported for K-Cu-Ce-Mg catalysts in the previous report (3Q, FY'96). Ethanol is a useful and simple probe molecule to test the metal and basic functions of isobutanol synthesis catalysts. Ethanol reactions, however, lead only to acetone and n-butyraldehyde (precursors to 2-propanol and 1-butanol, respectively), neither of which can form isobutanol precursors (e.g. isobutyraldehyde and propionaldehyde) during CO hydrogenation.

^{13}C-tracer studies of methanol/propionaldehyde cross-coupling reactions were carried out in order to examine chain-growth reaction pathways leading to C_4 oxygenates.

Catalysts (22 mg) were charged into a gradientless batch reactor. The samples were reduced in 10 % H_2 (balance He) at 623 K for 30 min. After the desired reaction temperature was reached, reactants were fed to the reactor. For the cross-coupling reactions of methanol and propionaldehyde on K-$CuMgCeO_x$ catalysts, the feed gas composition was $^{12}C_3H_6O/^{13}CH_3OH/CH_4/He$ = 4/8/2.7/86.6 kPa (methane was used as an internal standard). The reaction was carried out at 573 K and 101.3 kPa in the recirculating reactor unit (RRU). Products were sampled by syringe extraction from the recirculating stream at different contact times, and injected into a gas chromatograph equipped with flame ionization and thermal conductivity detectors. Mass spectrometry after chromatographic separation was used to confirm the identity of each reaction product.

Results of methanol and propionaldehyde cross-coupling reactions on low-Cu catalysts ($Cu_{0.5}Mg_5CeO_x$) are summarized as follows:

a) The conversion of methanol was comparable to that of propionaldehyde (Figure 1a). The turnovers of both methanol and propionaldehyde (moles converted per total number of Cu atoms) as a function of contact time are shown in Figure 1b.

b) Isobutyraldehyde, 1-propanol, and methyl propionate were the main reaction products (Figure 2).

c) Other products included CO (from methanol decomposition), CO_2 (from CO via water-gas shift reaction), methyl formate, 3-pentanone (propionaldehyde self-coupling followed by decarboxylation), 2-methyl-pentaldehyde (from propionaldehyde self-condensation) and 2-hydroxy-2-methyl-pentaldehyde. 2,2-Dimethyl butyraldehyde (from cross coupling of isobutyraldehyde and C_1 species) was not observed. Neither ethanol nor acetaldehyde formed during the cross-coupling reactions.

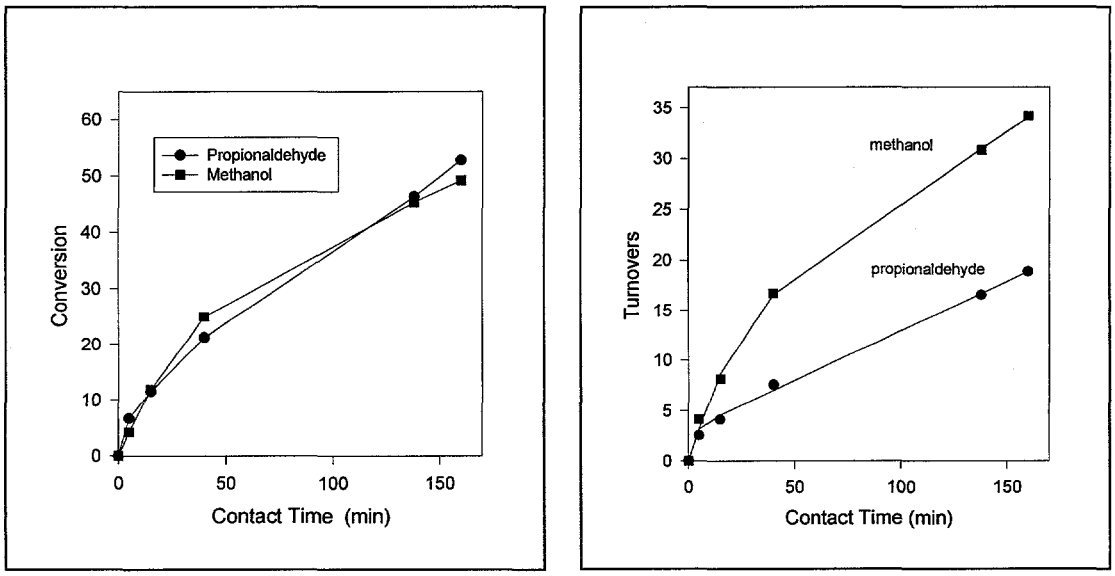

Figure 1. Methanol-propionaldehyde reactions on $Cu_{0.5}Mg_5CeO_x/K$ catalysts. (a) Methanol and propionaldehyde conversion as a function of contact time. (b) Methanol and propionaldehyde turnovers as a function of contact time.

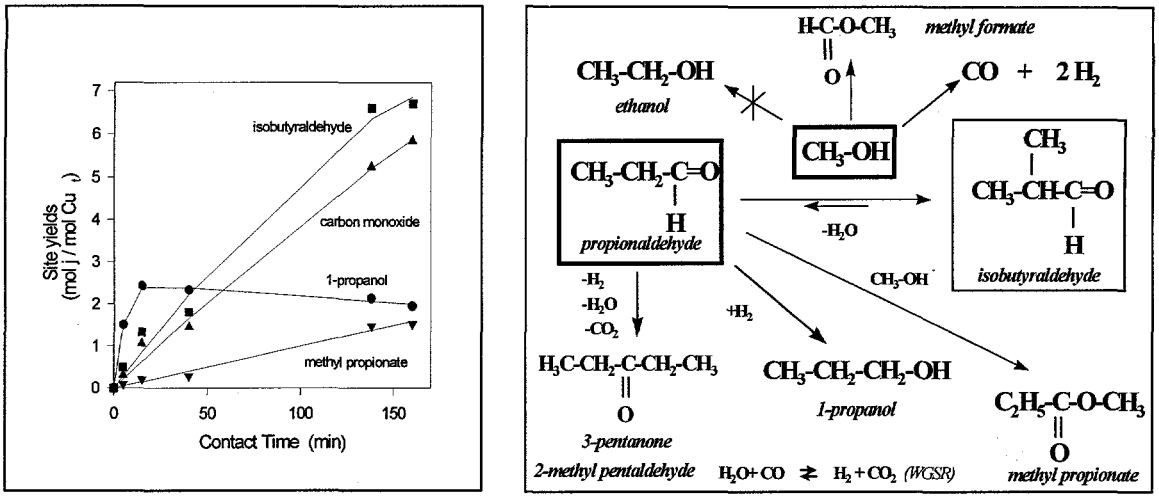

Figure 2. Methanol-propionaldehyde reactions. (a) Site yields as a function of contact time on $Cu_{0.5}Mg_5CeO_x/K$; (b) Simplified reaction scheme for methanol-propionaldehyde reactions.

Catalytic activity and product distributions obtained in methanol/propionaldehyde coupling reactions on high-Cu loading catalysts ($Cu_{7.5}Mg_5CeO_x/K$) are summarized as follows:

a) Methanol conversion was higher than that of propionaldehyde at all contact times (Figure 3a). The initial methanol turnover rate, calculated from the slope at zero contact time, was higher than that of propionaldehyde by a factor of two.

b) The reaction products are similar to those obtained on low-Cu catalyst with isobutyraldehyde, 1-propanol, methyl propionate, and CO_2 as the main products. The site-yields of these main products are shown in Figure 3b.

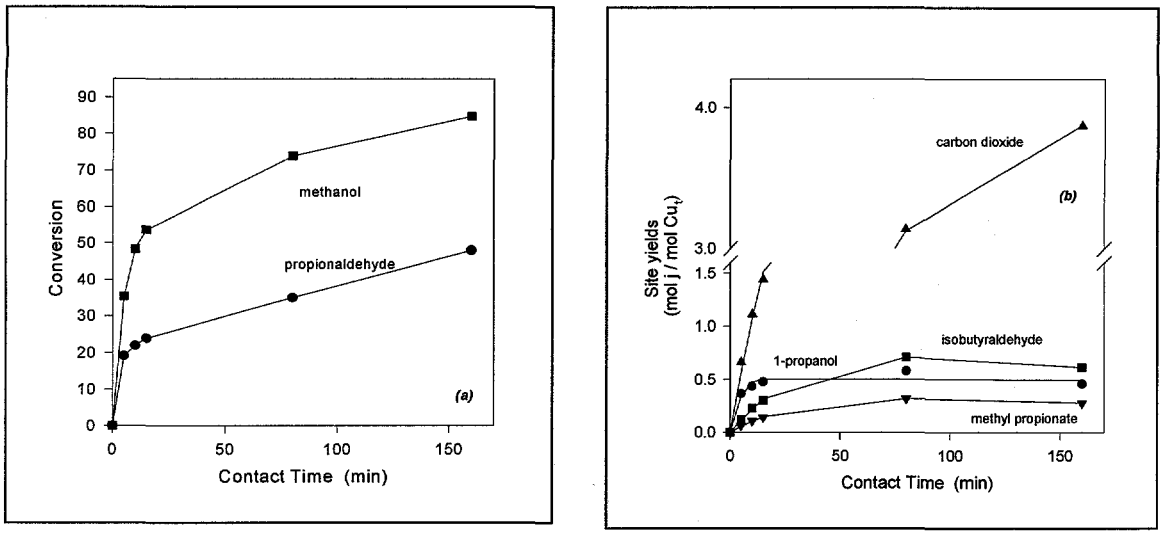

Figure 3. Methanol-propionaldehyde reactions on $Cu_{7.5}Mg_5CeO_x/K$ catalysts. (a) Methanol and propionaldehyde conversions as a function of contact time. (b) Site-yields as a function of contact time on $Cu_{7.5}Mg_5CeO_x/K$.

The methanol conversions obtained on MgO and Mg_5CeO_x were lower compared to that obtained on Cu-containing catalysts (Table 3 and Figure 4), but the propionaldehyde conversion was similar. The main reaction products were 1-propanol, 2-methyl-3-butenal, and isobutyraldehyde. The minor products included CO (from methanol decomposition), methyl propionate, and 3-pentanone.

Table 3. Effect of each catalyst component on the rates of methanol/propionaldehyde reactions.

Catalyst	$r_0^{methanol}$	$r_0^{propanal}$
MgO	1.1×10^{-5}	1.4×10^{-5}
Mg_5CeO_x	4.7×10^{-6}	9.1×10^{-6}
$Cu_{0.5}Mg_5CeO_x/K$	1.5×10^{-5}	1.1×10^{-5}
$Cu_{7.5}Mg_5CeO_x/K$	1.1×10^{-4}	5.5×10^{-5}

r_0 are expressed as mol / s . g_{cat}

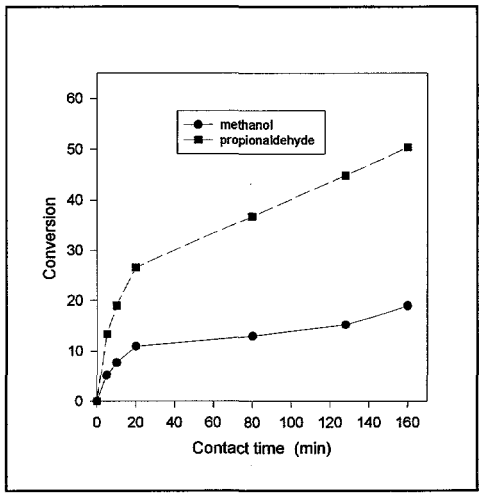

Figure 4. Methanol and Propionaldehyde conversions as a function of contact time on MgO.

Quantitative analysis of isotopic contents in products of ^{13}C-labeled methanol/propionaldehyde reactions was performed using a spreadsheet, which computes the ^{13}C contents in different molecules using a matrix deconvolution method [6]. The results obtained for ^{13}C-methanol/propionaldehyde reactions on K-$Cu_{0.5}Mg_5CeO_x$ are shown in Table 4. CO_2 molecules were predominantly labeled (87% ^{13}C) and formed from ^{13}CO via water-gas shift reactions. Unlabeled CO_2 was formed via the decarboxylation reactions leading to 3-pentanone (Figure 3b). Propionaldehyde acquired some^{13}C during reaction. The increment in the ^{13}C content of propionaldehyde molecules as a function of contact time can be explained by the scheme showed in Figure 5. The apparent presence of propionaldehyde with two ^{13}C atoms is an artifact caused by ^{18}O, which is present as an impurity in $^{13}CH_3OH$.

Table 4. Quantitative analysis of ^{13}C contents on reactant and products of $^{13}CH_3OH$/ $^{12}C_3H_6O$ cross-coupling reactions.

Time (min)	**0**	**5**	**10**	**20**	**40**	**80**
CO_2						
0		0.181	0.197	0.153	0.146	0.131
1		0.819	0.803	0.847	0.854	0.869
% ^{13}C		0.819	0.803	0.847	0.854	0.869
Propionaldehyde						
0	0.997	0.973	0.960	0.942	0.912	0.889
1	-0.001	0.008	0.013	0.022	0.032	0.047
2	0.004	0.018	0.025	0.034	0.051	0.059
3	0.000	0.001	0.002	0.003	0.004	0.005
% ^{13}C	0.002	0.016	0.023	0.033	0.049	0.060
Isobutyraldehyde						
0		0.064	0	0	0.039	0.039
1		0.849	0.927	0.874	0.810	0.800
2		0.064	0.052	0.087	0.099	0.101
3		0.024	0.021	0.034	0.044	0.050
4		0	0	0.005	0.008	0.009
% ^{13}C		0.261	0.273	0.293	0.293	0.298
Methyl propionate						
0			0	0	0.091	0.075
1			1.059	84.8	0.738	0.793
2			-0.061	0.057	0.057	0.041
3			0.002	0.096	0.116	0.093
4			0	-0.002	-0.002	-0.002
% ^{13}C			0.236	0.311	0.298	0.286

Isobutyraldehyde is predominantly labeled with one ^{13}C (Table 4), suggesting that it formed by cross-coupling reactions between ^{13}C-labeled methanol and propionaldehyde. Isobutyraldehyde with two ^{13}C atoms formed in the aldol condensation reaction of methanol ($^{13}C_1$ aldehyde-type intermediate) and propionaldehyde (with one

^{13}C). Methyl propionate contained mainly one ^{13}C atom. Both carbon atoms of methyl formate were labeled, indicating that it formed from two molecules of methanol.

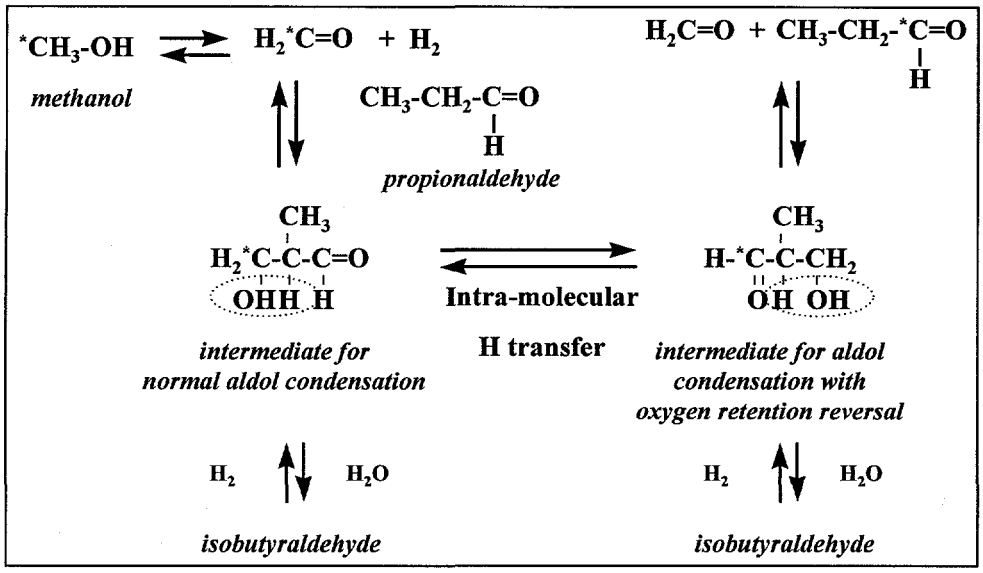

Figure 5. Reaction pathways leading to labeled propionaldehyde.

CH_3OH reactions were carried out in order to explore chain growth pathways leading to higher alcohols on base catalysts. In a typical experiment, the catalyst (18 mg) was charged into a gradientless batch reactor and reduced in 10 % H_2 (balance He) at 623 K for 30 min. After the desired reaction temperature was reached, reactants were fed to the reactor. For the methanol decomposition reaction on K-$CuMgCeO_x$ and MgO catalysts, the feed gas composition was $CH_3OH/CH_4/He$ = 4.0/2.7/94.6 (methane was used as an internal standard). The reaction was carried out at 573 K and 101.3 kPa in the recirculating reactor unit (RRU).

Results of methanol decomposition reactions on K-$Cu_{0.5}Mg_5CeO_x$ and MgO can be summarized as follows:

a) CO and H_2 were the most abundant products on both catalysts. The methanol conversions as a function of contact time are shown in Figure 6a. The methanol turnovers (moles converted per gram of catalyst) as a function of contact time on both K-$Cu_{0.5}Mg_5CeO_x$) and MgO are shown in Figure 6b. The initial rate is higher for copper-containing catalysts ($r_o = 7.6 \times 10^{-5}$ mol / g_{cat} s) than for pure MgO ($r_o = 4.0 \times 10^{-6}$ mol / g_{cat} s).

(b) In addition to CO and H_2, small amounts of methyl formate (from methanol condensation) and CO_2 (Figure 7a) were produced. CO_2 is formed from Boudouard reaction and/or methyl formate decomposition (Figure 7b). Ai and co-workers [6] studied the vapor-phase aldol condensation of formaldehyde with acetaldehyde over various metal oxides supported on silica gel. They found that the incorporation of an oxide of

transition metal, like CuO, promoted the formation of CH_3OH and formic acid. These two products are believed to form from HCHO via the process showed in Figure 7b. Basic sites favor the decomposition of formic acid to CO_2 and H_2 [7].

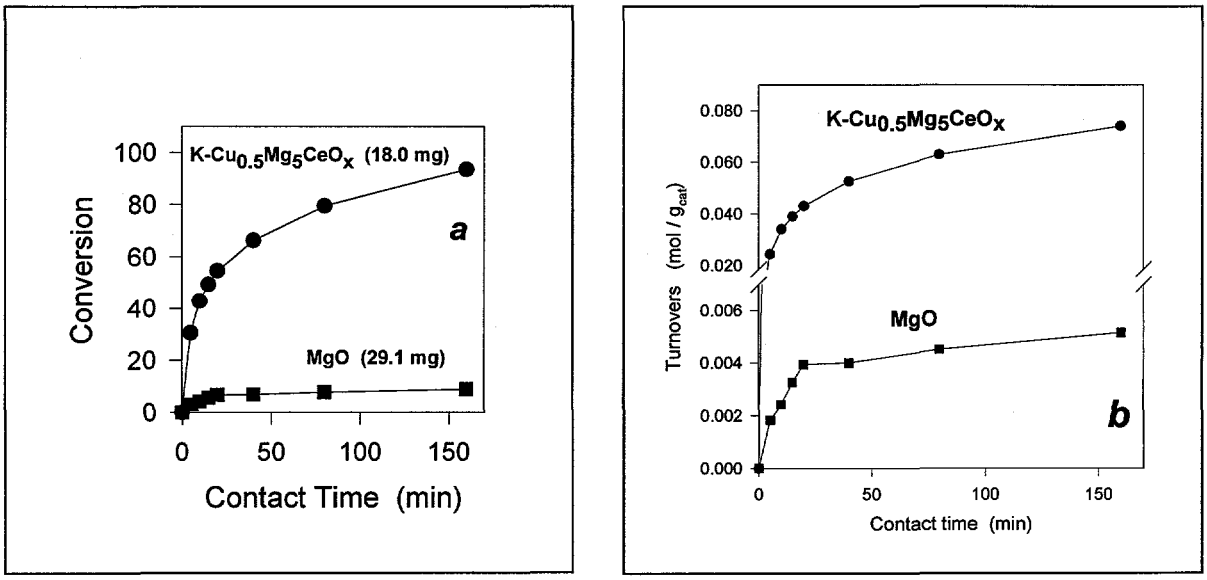

Figure 6. Methanol decomposition reaction on K-$Cu_{0.5}Mg_5CeO_x$ and MgO catalysts. (a) Methanol conversion. (b) Methanol turnovers.

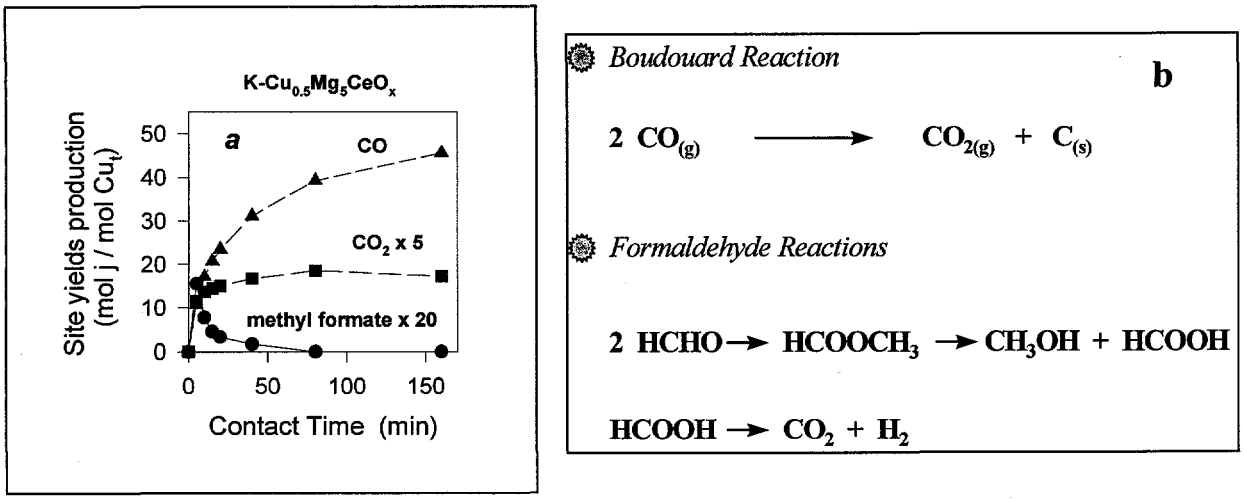

Figure 7. Methanol decomposition reaction on K-$Cu_{0.5}Mg_5CeO_x$. (a) Site-yields as a function of contact time; (b) Pathways of carbon dioxide production.

Methanol decomposition on Cu-based catalysts without using methane as internal standard was carried out in order to determined whether methane is produced from methanol under these conditions. The amount of methane produced was low (< 0.5%

selectivity). Alcohol decomposition occurs primarily through its dehydration or dehydrogenation on acidic or basic sites, respectively. In order to establish a correlation between the catalytic activity for methanol consumption and surface acid-base properties in MgO, Mg_5AlO_x and $MgAlO_x$, methanol dehydrogenation and dehydration reactions were investigated on these samples.

In a typical experiment, catalysts (30-40 mg) were charged into a gradientless batch reactor and pretreated in 10 % H_2 (balance He) at 623 K for 30 min. After the desired reaction temperature was reached, reactants were fed to the reactor. For the methanol decomposition reaction on $MgAlO_x$ and MgO catalysts, the feed gas composition was $CH_3OH/CH_4/He$ = 2.6/2.4/89.5 (methane was used as an internal standard). The reaction was carried out at 573 K and 101.3 kPa in the recirculating reactor unit (RRU).

Reaction rates, expressed as mol/g_{cat}-s, for each sample are shown in Figure 8. The initial rates of methanol consumption along with the catalyst properties are summarized in Table 5. CO_2, CO and H_2 were the only products, and DME and hydrocarbons were not formed on pure MgO. CO_2 formed via methyl formate decomposition [8,9] or from carbonaceous deposits (C_nH_x oxygen deficient compounds) that remained on the surface. On Mg_5AlO_x and $MgAlO_x$ samples, DME, CO_2, and CO were detected. DME was formed via dehydration of methanol on acid sites [8,9].

Table 5. Properties and rates of methanol conversion.

Catalyst	Al/Mg	K wt. %	S.A. m^2 / g	$^{13}CO_2/^{12}CO_2$ exchange at 573 K x 10^{-6} μmol / m^2	r_0 mol / g_{cat}-s	r_0 mol / m^2-s
MgO	0	0.2	194	0.38	4.0×10^{-6}	2.1×10^{-8}
Mg_5AlO_x	0.2	0.02	184	0.10	2.7×10^{-6}	1.5×10^{-8}
$MgAlO_x$	1	0.08	230	0.21	4.7×10^{-6}	2.0×10^{-8}

r_0 is the rate of methanol consumption, and is expressed in mol/g_{cat}.s or mol/m^2 total.s.

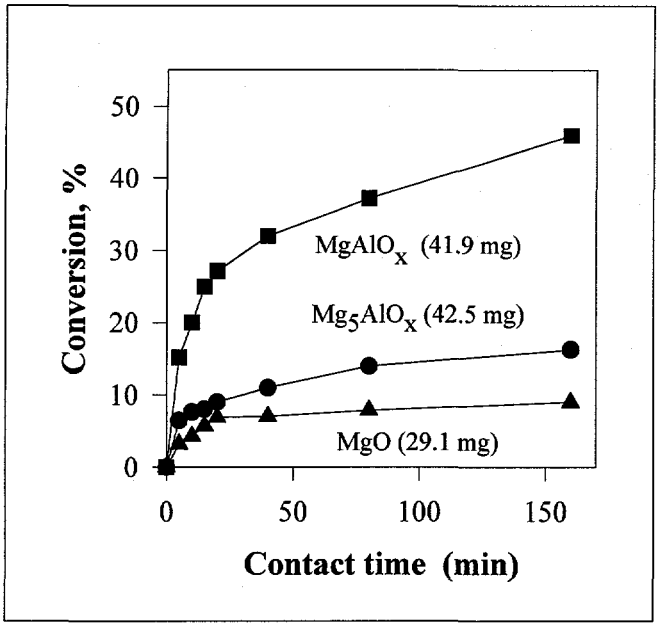

Figure 8. Methanol conversion as a function of contact time on different $MgAlO_x$ catalysts. [T_r=573 K, $P_{methanol}$=2.6 kPa, P_T=101.3 kPa].

The ratio of the initial rates of DME and CO_x formation as a function of Mg/Al ratio on different Mg-Al samples is shown in Figure 9. The DME/CO_x ratio increases monotonically with increasing Al content. This ratio reflects the relative number of acid and basic sites in the catalyst. Acid sites lead to DME and basic sites are responsible for CO_x formation. For $MgAlO_x$, the amount of DME produced is higher than CO_2 and CO; whereas less DME and more CO_x formed on Mg_5AlO_x than on $MgAlO_x$, suggesting $MgAlO_x$ is less basic and more acidic than Mg_5AlO_x. DME was only observed on Al-containing MgO samples, suggesting that Al cations increase the acidity of MgO.

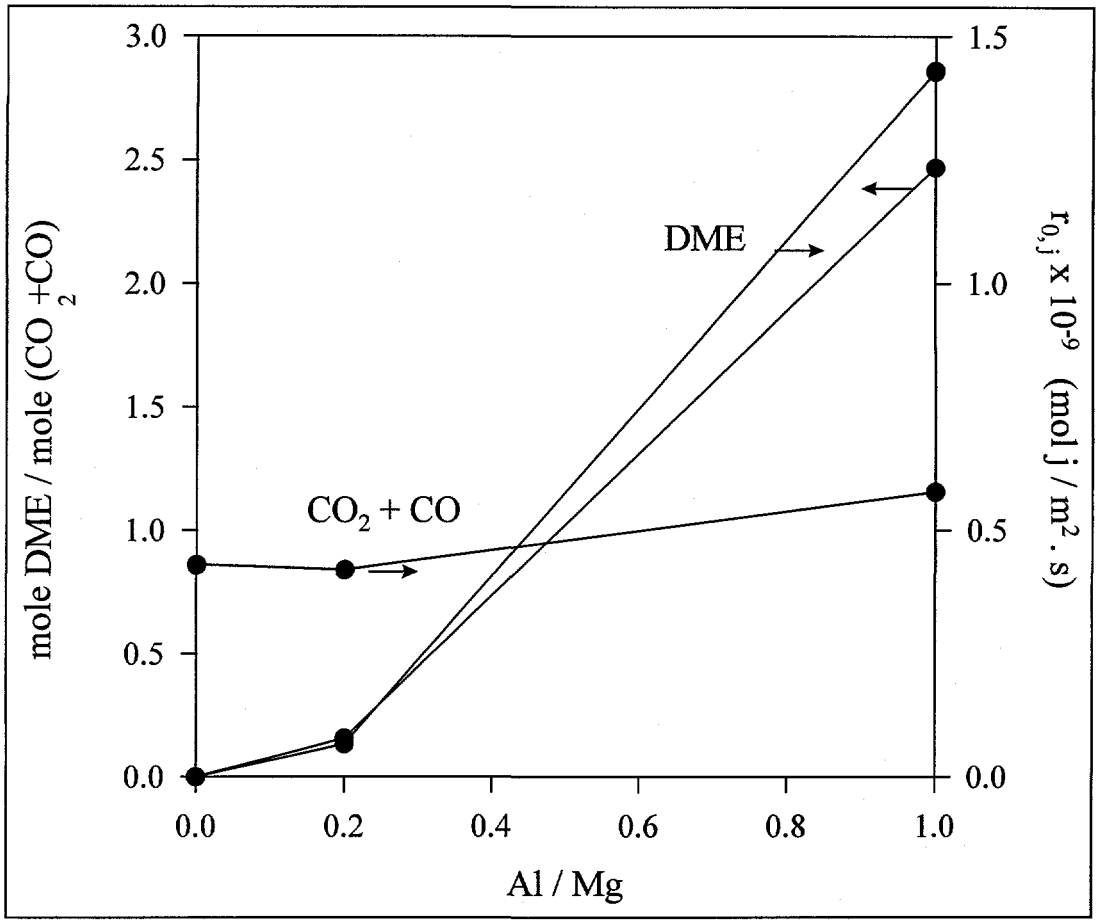

Figure 9. Methanol reaction on $MgAlO_x$ catalysts: Effect of Mg/Al ratio on product distribution. [T_r=573 K, $P_{methanol}$=2.6 kPa, P_t=101.3 kPa].

In recent Amoco patents [10,11], the following reaction was carried out on modified MgO catalysts for the synthesis of higher alcohols from methanol in the presence of ethylene:

$$C_2H_4 + CH_3OH \longrightarrow C_3H_7OH \xrightarrow{CH_3OH} \text{isobutanol}$$

It is known that SAPO-34 (acid catalyst) converts methanol to olefins (selectivity higher than 80% to $C_2^=$ and $C_3^=$) and MgO (base catalyst) catalyzes the condensation reactions between olefins and methanol to produce isobutanol [10,11]. It is possible to produce 1-propanol and isobutanol from methanol in one step by using a physical mixture of SAPO-34 and Mg_5CeO_x. To verify this, a physical mixture of SAPO-34 (6.7 mg) and Mg_5CeO_x (26.2 mg) was charged into a gradientless batch reactor and pretreated in 10 % H_2

(balance He) at 623 K for 30 min. The feed gas composition was CH_3OH/He = 5.8/90.0 kPa. The reaction was carried out at 623 K and 101.3 kPa in the recirculating reactor unit (RRU). The results are summarized in Figure 10.

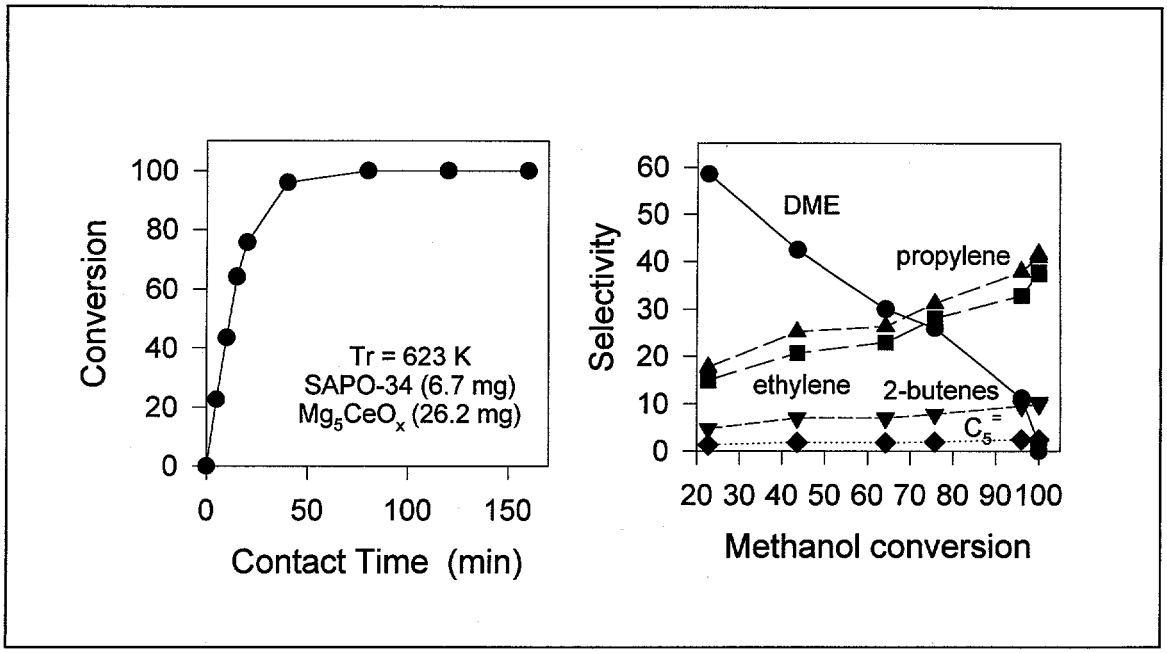

Figure 10. Methanol reactions on a physical mixture of SAPO-34/Mg_5CeO_x (6.7/26.2 mg). a) Methanol conversion vs. contact time, b) product selectivity vs. methanol conversion [T_r=623 K, $P_{methanol}$=5.8 kPa, P_t=101.3 kPa].

Methanol was predominantly converted to propylene and ethylene. Other products included DME, CO, CO_2, methane, ethane, propane, butane, pentane, 1-butene, 2-butene, and 1-pentene. The product distribution was similar to that obtained on pure SAPO-34 catalyst charge and no alcohols were detected. Neither isobutanol nor its precursor was observed. Methanol conversion to olefins was much faster than condensation reactions between olefins and C_1 intermediate species.

Future work in the alcohol coupling reactions includes:

1. Competitive reactions between $^{13}CH_3$-^{13}CHO and CH_3CH_2OH, to explain the rate of acetone in ethanol dehydrogenation and coupling reactions on $Cu_{0.5}Mg_5CeO_x$ catalyst.
2. Reactions of $^{13}CH_2O$ with acetaldehydes on different catalysts to explore the chain-growth ability of different materials.
3. Reactions between $^{13}CH_2O$ and CH_3CH_2CHO on $Cu_{0.5}Mg_5CeO_x$ catalysts.
4. ^{13}C-tracer studies of methanol-acetaldehyde (or methanol-propionaldehyde) cross-coupling reactions in order to examine reaction pathways leading to chain growth and C_3 oxygenates on catalytic materials described in the synthesis section.

3. Isobutanol Synthesis at High Pressure in CMRU

A $Cu_{0.5}Mg_5O_x$ catalyst was examined in the synthesis of isobutanol from CO/H_2 at 593 K and 4.5 MPa and space velocities between 6000-1000 cm^3 (STP)/ g-cat.h. The results are presented in Figure 11a and Table 6. As a comparison, the results obtained on K-$Cu_{0.5}Mg_5CeO_x$ (MG3-11Ow/K) are also given in Figure 11b and Table 6.

CO conversion on $Cu_{0.5}Mg_5O_x$ increases with increasing bed residence time; methanol is the major product followed by paraffins, isopropanol, ethanol, and propanol. CO conversion rates decrease with increasing bed residence time, suggesting a gradual approach to methanol synthesis equilibrium. Methanol selectivity decreases and isobutanol selectivity increases with increasing bed residence time, suggesting that methanol is a reaction intermediate that undergoes further reactions at longer bed residence times leading to higher alcohols, such as isobutanol. $Cu_{0.5}Mg_5O_x$ catalysts show high hydrocarbon and low isobutanol selectivities compared to K-$Cu_{0.5}Mg_5CeO_x$, consistent with the lower basicity of the K-free catalyst. The $^{13}CO_2/^{12}CO_2$ isotopic exchange results indicate that a greater number of basic sites are available on K-$Cu_{0.5}Mg_5CeO_x$ compared to $Cu_{0.5}Mg_5O_x$ (Table 7). Moreover, the strength of these available basic sites are stronger on K-$Cu_{0.5}Mg_5CeO_x$. Strong basic sites lead to higher isobutanol production rates. Isobutanol production increases with increasing bed residence time, suggesting 1) isobutanol is a secondary reaction product and 2) CO_2, one of the reaction product, does not inhibit isobutanol formation on $Cu_{0.5}Mg_5O_x$ as strongly as on K-$Cu_{0.5}Mg_5CeO_x$ because of the weaker basicity of the former. Methanol turnover rates on $Cu_{0.5}Mg_5O_x$ (7.0×10^{-3} CH_3OH/surface Cu.s) are higher than on K-$Cu_{0.5}Mg_5CeO_x$ (4.6×10^{-3} CH_3OH/surface Cu.s), suggesting that the active site (Cu) for methanol synthesis on K-$Cu_{0.5}Mg_5CeO_x$ is inhibited by reaction products such as CO_2 and H_2O. The Cu atoms in K-$Cu_{0.5}Mg_5CeO_x$ are more likely to be oxidized by CO_2 and/or H_2O because of the small Cu crystallites (Table 7) and strong interaction between Cu and CeO_x.

As mentioned earlier, a large batch of 1.0 wt % K-$Cu_{0.5}Mg_5CeO_x$ catalyst has been prepared recently. This catalyst will be tested again for the synthesis of isobutanol from CO/H_2 and used in future studies of alcohol-chain growth reactions. This run will consist of 1) variation in space velocity, 2) addition of 1-propanol, 3) addition of ethanol, 4) addition of CO_2, and 5) changes in reaction temperatures. The gas chromatograph TCD and FID will also be recalibrated using a mixture containing Ar, He, N_2, CO, CO_2, methane, ethane, ethylene, propane, propylene, acetylene, methanol, ethanol, and DME.

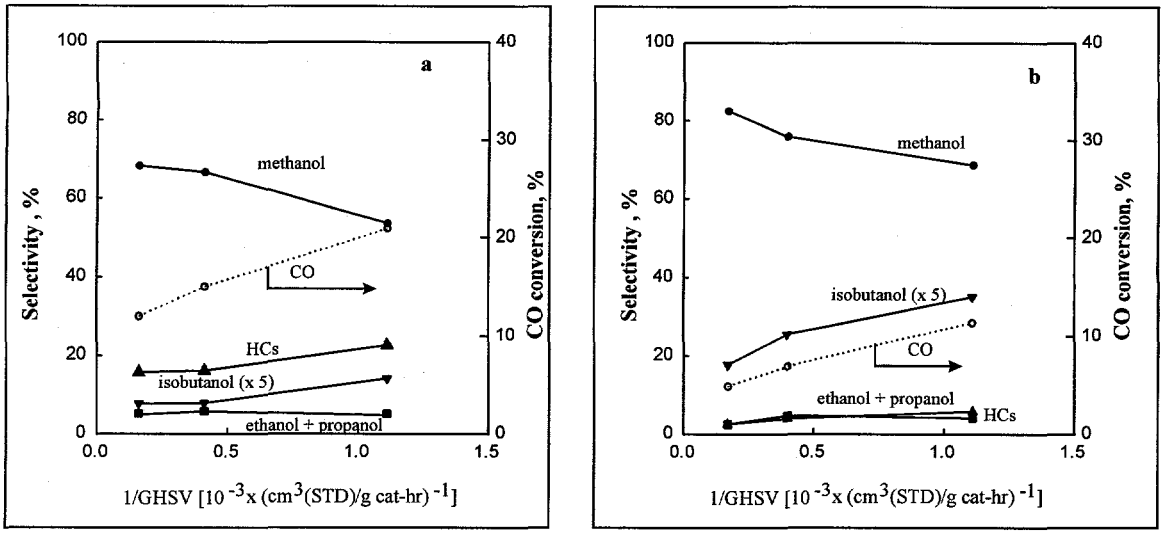

Figure 11. CO conversion and product selectivities vs. space velocity on a) $Cu_{0.5}Mg_5O_x$ and b) 1.1 wt % K-$Cu_{0.5}Mg_5CeO_x$. (593 K, 4.5 MPa, CO/H_2 =1).

Table 6. Product selectivities and methanol turnover rates on $Cu_{0.5}Mg_5O_x$ (CMRU-22) and K-$Cu_{0.5}Mg_5CeO_x$ (CMRU-20).

Catalyst	$Cu_{0.5}Mg_5O_x$	$Cu_{0.5}$ Mg_5O_x	K-$Cu_{0.5}Mg_5CeO_x$
GHSV [cm^3/g cat. h]	903	6262	903
CO conversion [%]	20.9	12.0	11.4
Methanol turnover rate [$mol_{Methanol}/mol_{Surface\ Cu\text{-}S}$]	7.0	37.2	4.6
Product selectivities [%]			
Methanol	53.6	68.3	68.7
Ethanol+propanol	5.1	5.1	4.1
isobutanol	2.8	1.6	7.0
CO_2	18.8	12.3	22.3
Paraffins	22.6	15.8	5.8

Reaction conditions: 593 K, 4.5 MPa, H_2/CO=1, 2.06 g catalyst.

Task 4: Identification of Reaction Intermediates

4.1. Determination of Copper Surface Area

The decomposition of N_2O has been used to measure Cu surface areas on K-$CuMgCeO_x$ catalysts. All these catalysts have been pre-reduced at 623 K in 5 % H_2/He. The decomposition of N_2O on reduced ZnO support sites has been found to contribute significantly to the overall Cu surface area on Cu/ZnO catalysts [12]. It is possible that the decomposition of N_2O on the reduced CeO_x species in pre-reduced $CuMgCeO_x$ catalysts also corrupts N_2O titration and leads to overestimates of copper dispersion. Our previous studies have shown that N_2O is not consumed on Cu-free $MgCeO_x$ samples pre-reduced at 623 K, suggesting that CeO_x remains in its full oxidation state during H_2 treatment. This observation, however, cannot rule out the possibility that CeO_2 may

reduce when Cu is available to dissociate H_2 in Cu-containing $MgCeO_x$ samples. In effect, the presence of Cu may promote the reduction of CeO_2.

In order to rule out any contributions from reduced CeO_x species to N_2O titration measurements of Cu surface area, a reduction-oxidation cycle was performed. A $Cu_{0.5}Mg_5CeO_x$ sample was reduced at 623 K and N_2O titration data at 363 K were obtained. The measured Cu surface area was found to be 19.0 m^2/g-cat (23 % Cu dispersion). This sample was re-reduced at 473 K instead of 623 K. Surface oxygen atoms on Cu surface can be removed at 473 K in H_2, but reduction of CeO_2 is likely to occur only at much higher reduction temperatures. Thus, reduction at 473 K is likely to remove oxygen from Cu surface but not from CeO_x. The Cu area of the sample reduced at 473 K was 19.3 m^2/g-cat, which is very similar to the value of 19.0 m^2/g-cat obtained on the fresh sample after reduction at 623 K. This demonstrates that CeO_x does not contribute to the measured copper dispersion and that these high dispersion values indeed reflect the presence of small Cu metal crystallites (about 5 nm). An additional exposure of this titrated sample to 5 % H_2/He at 423 K resulted in a Cu surface area of 17.9 m^2/g-cat, suggesting that oxygen atoms chemisorbed on Cu can be almost completely removed by H_2 at temperatures as low as 423 K.

4.2. Determination of Basic Site Density and Strength

The density and strength of basic sites were measured from the exchange capacity and rates obtained in a $^{13}CO_2/^{12}CO_2$ isotopic exchange method developed as part of this project; this method provides a direct measure of the number of basic sites *"kinetically available" at reaction temperatures*. In addition, this technique provides a measure of the distribution of reactivity among available basic sites. In this method, a pre-reduced catalyst (50 mg) is exposed to a 0.1 % $^{13}CO_2$/0.1 % Ar/He stream (100 cm^3/min) and after $^{13}CO_2$ reached a constant level in the effluent, the flow is switched to 0.1 % $^{12}CO_2$/He (100 cm^3/min). The relaxation of the $^{13}CO_2$ displaced from the surface is followed by mass spectrometry. In contrast with CO_2 temperature programmed desorption (TPD), $^{13}CO_2/^{12}CO_2$ exchange methods probe the density and reactivity of reactive basic sites at reaction temperatures and chemical equilibrium, without contributions from unreactive carbonates and without disrupting the steady-state coverage on catalytic solids.

Figure 12 shows the transients obtained on a $Cu_{0.5}Mg_5CeO_x$ catalysts when the isotopic composition of CO_2 was switched at 573K. As $^{13}CO_2$ was switched to $^{12}CO_2$ at zero time, without altering the partial pressure or flow rate of CO_2, the concentration of $^{13}CO_2$ decreases as $^{12}CO_2$ concentration increases and the total gas phase concentration of CO_2 (i.e., $^{12}CO_2 + {}^{13}CO_2$) remains constant. The presence of Ar as an inert tracer permits correction for gas holdup and hydrodynamic delay in the apparatus.

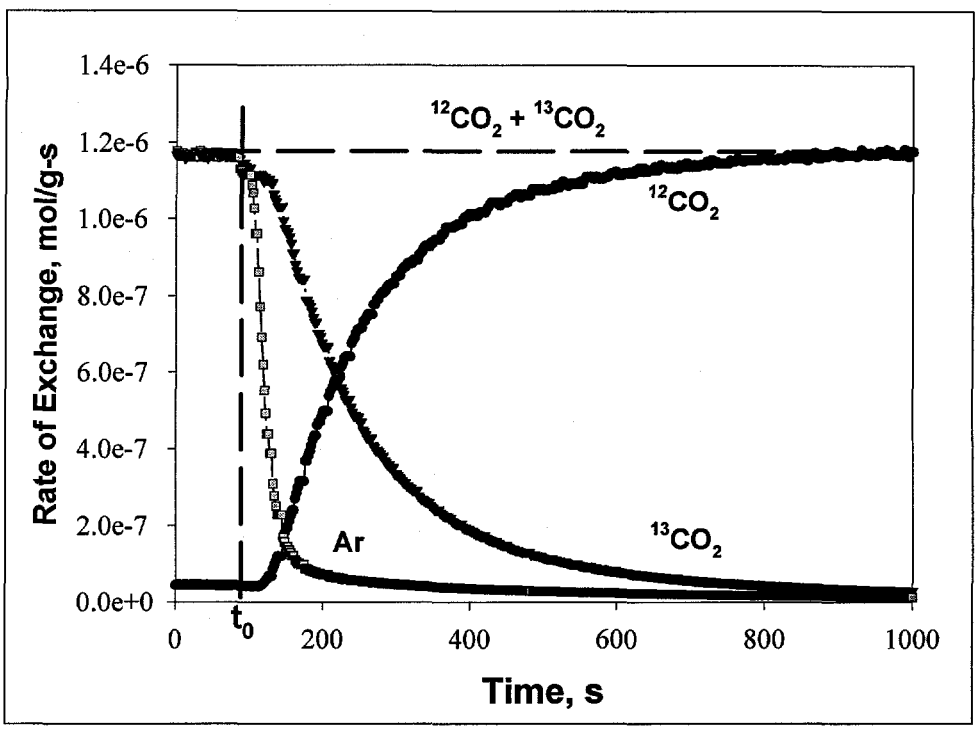

Figure 12. Steady-state transients observed for $Cu_{0.5}Mg_5CeO_x$ upon switching from $^{13}CO_2$/He to $^{12}CO_2/H_2$ at 573 K.

The significant delay in the steady-state transient of $^{13}CO_2$, relative to Ar curve, indicates that the former originates from catalyst-bound $^{13}CO_2$ species that desorb slowly at the temperature of the isotopic exchange experiment. The coverage or number of surface CO_2 species remains constant, i.e.,

$$\theta_{^{13}CO_2\,(t=0)} = \theta_{^{13}CO_2\,(t)} + \theta_{^{12}CO_2\,(t)} = \theta^{total}_{CO_2\,(t)} = \theta_{^{12}CO_2\,(t=\infty)}$$

At $t=t_0$, the surface is only covered by $^{13}CO_2$ and at a longer time after the switch, the surface is predominantly occupied by $^{12}CO_2$. Therefore, the amount of $^{13}CO_2$ displaced from the surface by $^{12}CO_2$ reflects the exchange capacity of the catalyst at the reaction temperature. The exchange capacity is determined from the area under the $^{13}CO_2$ curve (Figure 12). This area, properly corrected for the response factor of the mass spectrometer and gas holdup, corresponds to the number of basic sites that participate in exchange reactions at 573 K. The number of basic sites (exchangeable CO_2) kinetically available for exchange experiments on MgO, CeO_2, and K-, CeO_x- and AlO_x- modified MgO samples are shown in Table 7. Weakly interacting sites are mostly unoccupied by CO_2 and strongly interacting sites do not exchange in the time scale of the isotopic relaxation experiment. These strongly interacting sites and weakly interacting sites are also unlikely to contribute to catalytic reactions at similar temperatures.

As a comparison, the number of basic sites determined from CO_2 temperature programmed desorption (TPD) measurements based on the amount of CO_2 released at temperature below 573 K are also given in Table 7. In this method, CO_2 is adsorbed on the pre-reduced catalyst (50 mg) at room temperature for 10 min. The catalyst surface is subsequently flushed with He (100 cm^3/min) to remove gas phase and weakly adsorbed CO_2 before linearly ramping the temperature at 0.5 K/s, and measuring the CO_2 desorption profile by mass spectrometry. The area below the TPD curve was used to measure the number of CO_2 molecules desorbed, and the number of basic sites on the metal oxide surface was calculated using a 1:1 CO_2 / basic site stoichiometry.

Table 7. Composition, surface area, and basic site density of mixed metal oxides

[a]Sample	[b]Sg, m^2/g	[c]Cu, dispersion, %	Exchangeable CO_2 at 300 °C 10^{-6} mol/m^2	CO_2 desorbed during TPD at T < 300 °C 10^{-6} mol/m^2
MgO	191	/	0.38	0.50
CeO_2	80	/	0.92	/
K-Mg_5CeO_x	188	/	0.95	0.84
$Cu_{0.5}Mg_5O_x$	118	6	0.40	/
0.1 wt% K-$Cu_{0.5}Mg_5CeO_x$	167	23	1.20	0.62
1.1 wt% K-$Cu_{0.5}Mg_5CeO_x$	147	14	2.33	0.64
3.5 wt% K-$Cu_{0.5}Mg_5CeO_x$	62	6	5.22	0.65
1.2 wt % K-$Cu_{7.5}Mg_5CeO_x$	92	5	3.17	0.91
Cs-Cu/ZnO/Al_2O_3	62	/	1.09	0.62

[a] Bulk composition measured by atomic absorption.
[b] Total surface area determined by N_2 BET adsorption at 77 K.
[c] Dispersion calculated from the ratio of surface Cu (determined by N_2O decomposition at 90 °C [13, 14]) to the total number of Cu atoms in the catalyst.

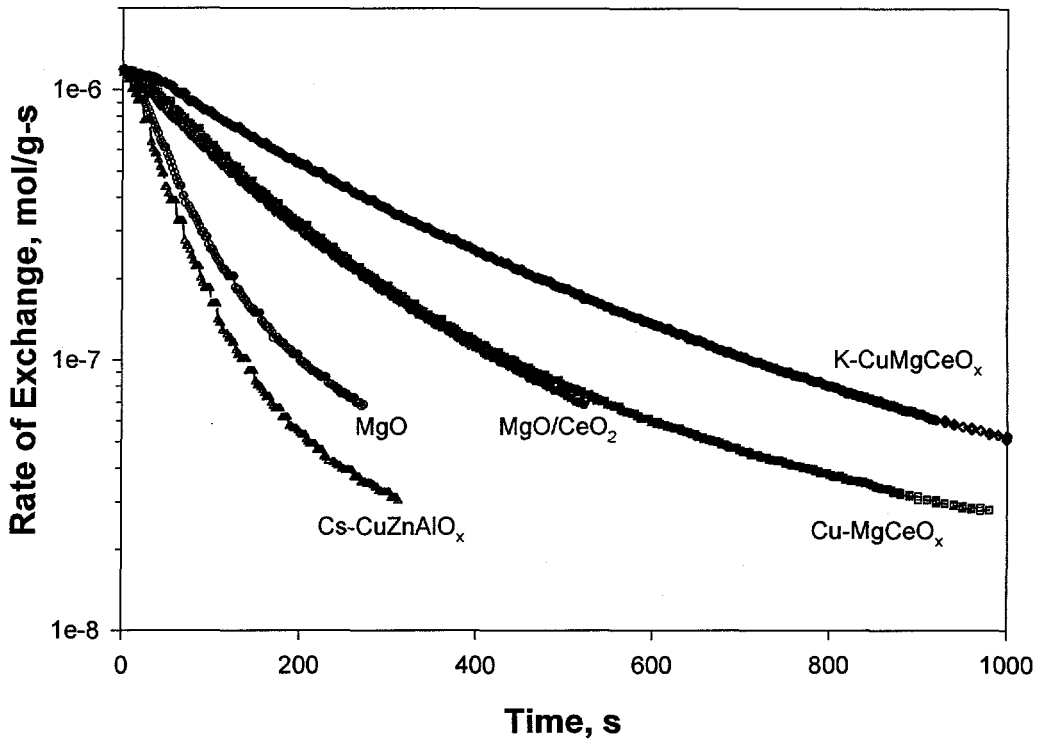

Figure 13. The transient response observed for mixed oxides upon switching from $^{13}CO_2$ to $^{12}CO_2$: T = 573 K.

The local slope in the semi-logarithmic plots of Figure 13 reflects the dynamics of the first-order CO_2 exchange reaction and thus the exchange rate constant on available basic sites. The curved semi-logarithmic plots show that $Cu_{0.5}Mg_5CeO_x$ surfaces contain sites with a broad distribution of exchange rate constants, because uniform surfaces with only one type of adsorption site would lead to linear plots in Figure 13. Exchange rate constants depend on the thermodynamics of binding interactions between CO_2 and basic sites through linear free energy relations commonly used to estimate activation energies for chemical reactions [15]. Large exchange rate constants and the concomitant short relaxation times (*e.g.* on MgO and Cs-Cu/ZnO/Al_2O_3) reflect shorter CO_2 surface lifetimes and weaker binding of CO_2 molecules on available basic sites.

The distribution of exchange rate constants was obtained for each catalyst sample from the relaxation dynamics using inverse Laplace transform deconvolution methods [16]. These distributions of exchange kinetic constants are shown in Figure 14. The distribution curves were normalized to give an area of unity. The y-axis represents the distribution function f(k), where f(k)dk is defined as the fraction of the total number of kinetically accessible basic sites with exchange rate constants between k and k+dk. The logarithmic rate constant in the x-axis of Figure 14 can be related to an activation energy for exchange if we assume that the pre-exponential factors for adsorption-desorption rate constants are not influenced by basic strength:

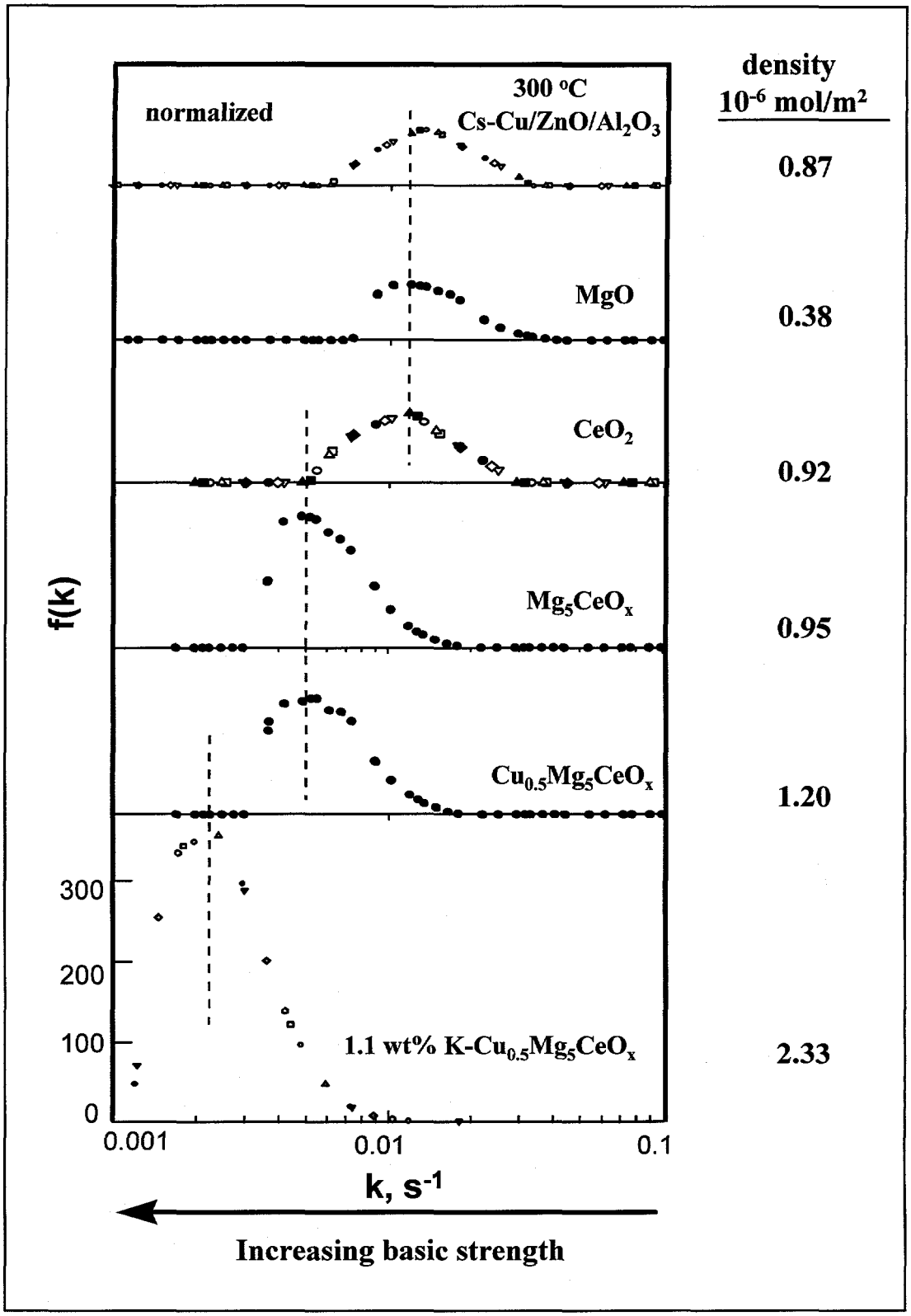

Figure 14. Basic strength distribution with respect to exchange rate constant for mixed metal oxides.

$$\log k = \log [A \exp (-E/RT)] = \log A - (2.3\ E/RT)$$

The use of linear free energy relations between the activation energy and the enthalpy of adsorbed CO_2 :

$$E = E_o - \alpha \Delta H_{ads}$$

preserves the linear dependence between the logarithm of k and the enthalpy of CO_2 adsorption; the latter is directly related to the basic strength of surface sites on MgO-based solids.

As shown in Table 7, the surface density of available basic sites on MgO at 573 K is 0.38 x 10^{-6} mol/m^2. This site density is much lower than the value of 18.3 x 10^{-6} mol/m^2 reported for MgO surface oxygen density [17], and it corresponds to about 2.1 % of these surface lattice oxygen in MgO acting as basic sites available for $^{13}CO_2/^{12}CO_2$ isotopic exchange reaction at 573 K. This number (2.1 %) is lower than the values reported by Davis et al. [17] (25 %) and Kurokawa et al. [18] (10 %) using CO_2 TPD. This is not unexpected since the $^{13}CO_2/^{12}CO_2$ isotopic switch method only probes the number of basic sites that participate in the exchange reactions near 573 K. Weakly basic sites are mostly unoccupied by CO_2 and strongly interacting basic sites do not exchange in the time scale of isotopic exchange experiment. The number of basic sites given by Davis and Kurokawa, however, include both weak and strong basic sites that are not detected by the isotopic exchange method. Neither strong nor weak basic sites are likely to contribute to catalytic reactions at temperatures similar to those of the isotopic switch experiments. The CO_2 TPD results shown in Table 7 do not reflect the total but the number of basic sites that release CO_2 below 573 K. It should be pointed out that the basicity of MgO depends strongly on the source, purity, preparation procedures, and calcination temperatures of MgO [19-21]. All these variables affect the concentrations of surface OH species (less basic) and coordinately unsaturated oxygen (O_{cus}) sites like kinks, steps, corners, and edges.

Basic site densities in CeO_2 determined by either isotopic exchange or CO_2 TPD method are higher than on MgO (Table 7). In fact, the *available basic sites at 573 K* in CeO_2 are stronger compared those in MgO as evidenced by the lower exchange rate constants on CeO_2 (Figure 14). This does not necessarily mean that CeO_2 is a stronger base than MgO, because the stronger basic sites on MgO are not probed by $^{13}CO_2/^{12}CO_2$ exchange experiment at 573 K. $^{13}CO_2/^{12}CO_2$ exchange experiments carried out on a CeO_x sample without 5 % H_2/He reduction at 623 K show a similar density of basic sites and strength compared to the sample subject to H_2 treatment, suggesting that H_2 treatment at 623 K did not affect the properties of available basic sites at 573 K.

The presence of small amounts of CeO_x in MgO (Mg/Ce = 5) increases both the density (Table 7) and strength (Figure 14) of basic sites kinetically accessible for exchange reactions at 573 K. Similar phenomena have been reported by Rane et al. [22] using a CO_2 temperature programmed desorption. These authors observed a marked

increase in the number of both weak and strong basic sites per gram of catalyst upon addition of ceria to MgO. The electron density and consequently the basicity of oxygen ions associated with both Ce^{4+} and Mg^{2+} cations are expected to be different from the ones bounded to only Ce^{4+} or Mg^{2+} ions. As mentioned early, MgO surfaces may have a high density of very strong basic sites that are not probed by $^{13}CO_2/^{12}CO_2$ exchange nor involved in catalytic reactions near 573 K. The presence of Ce^{4+} ions, because of their higher electron affinities compared to Mg^{2+} ions, tend to attract electrons from the oxygen ions associated with Mg^{2+}, resulting in a decrease in *electron* density and basic strength of these oxygen ions and therefore making them available for exchange (and catalysis) at 573 K. The increase in basic site density and strength might also be due to the creation of low-coordinated oxygen ions in the boundary region of these two oxides.

The presence of Cu in $MgCeO_x$ samples slightly increase the basic site density (Table 7) but does not modify the basic strength distribution (Figure 14). Ikawa and co-workers [18] have also reported recently that the distribution of surface basicity on MgO is not modified by the presence of Cu^{2+} ions even though the basic site density increased significantly. They proposed that the larger Cu^{2+} ion is introduced into the MgO lattice, which causes a distortion in the lattice and leads to an increase in the Mg-O bond length and in the localization of electrons near the oxygen ions. In this case, we would expect, however, a change in the distribution of basic site strength. The slightly increase in basic site density in $Cu_{0.5}Mg_5CeO_x$ compared to Mg_5CeO_x may result instead from the contribution of adsorption sites associated with Cu^{2+} ions because Cu metal in the pre-reduced sample could be oxidized by CO_2 during the $^{13}CO_2/^{12}CO_2$ exchange experiment at 573 K. In fact, during CO_2 temperature programmed desorption experiments where Cu is likely to remain metallic, the number of basic sites is lower in $Cu_{0.5}Mg_5CeO_x$ than in Mg_5CeO_x.

The addition of K (1.1 wt %) increases not only the density of basic sites on $Cu_{0.5}Mg_5CeO_x$ (Table 7), but also their strength, as shown by the shift in the distribution to lower exchange rate constants (Figures 14). An increase in K loading from 1.1 to 3.5 wt % increased basic site density from 2.3 to 5.2×10^{-6} m^2/g, but essentially had no effect on the exchange rate constant distribution. Because of the lower electron affinity of K^+ compared to Mg^{2+}, the oxygen ion of K_2O has a higher negative charge, and therefore is more basic than that of MgO. Moreover, the oxygen ions connected with both K^+ and Mg^{2+} ions are expected to have higher electron density compared to ones associated with only Mg^{2+}, resulting in the formation of stronger basic sites in MgO.

Calcination of hydrotalcite (magnesium-aluminum hydroxycarbonate) results in a mixed-oxide solid solution with high surface area and high thermal and hydrothermal stability. This material is active for base-catalyzed reactions, including aldol-condensation and double bond isomerization reactions [23,24]. Stork and co-workers [24] used Hammett indicators and the kinetics of double-bond isomerization to suggest that $MgAlO_x$ oxides exhibit strong basic sites similar to those of pure MgO. McKenzie et al. [17] using temperature-programmed desorption of CO_2 and the decomposition of 2-propanol and Dumesic et al. [25] using microcalorimetric measurement of CO_2 heat of

adsorption suggested that $MgAlO_x$ mixed-metal oxides are less basic than pure MgO. In this study, the basicity of $MgAlO_x$ mixed-metal oxides was measured by using both temperature-programmed desorption of CO_2 and $^{13}CO_2/^{12}CO_2$ isotopic exchange methods and the results are shown in Table 8.

Table 8. Composition, surface area, basic site density of mixed metal oxides

Sample	K, wt %	Surface area (m^2/g)	$^{13}CO_2/^{12}CO_2$ exchange at 573 K $\mu mol/m^2$	$^{13}CO_2/^{12}CO_2$ exchange at 473 K $\mu mol/m^2$	$^{13}CO_2$ TPD at T < 573 K $\mu mol/m^2$	$^{13}CO_2$ TPD T< 723 K $\mu mol/m^2$
$MgAlO_x$	0.08	230	0.21	0.25	0.50	0.66
Mg_3AlO_x	0.02	238	0.17	0.21	0.34	0.50
Mg_5AlO_x	0.02	184	0.10	0.09	0.30	0.41
MgO	/	125	0.35	0.43	1.17	1.50

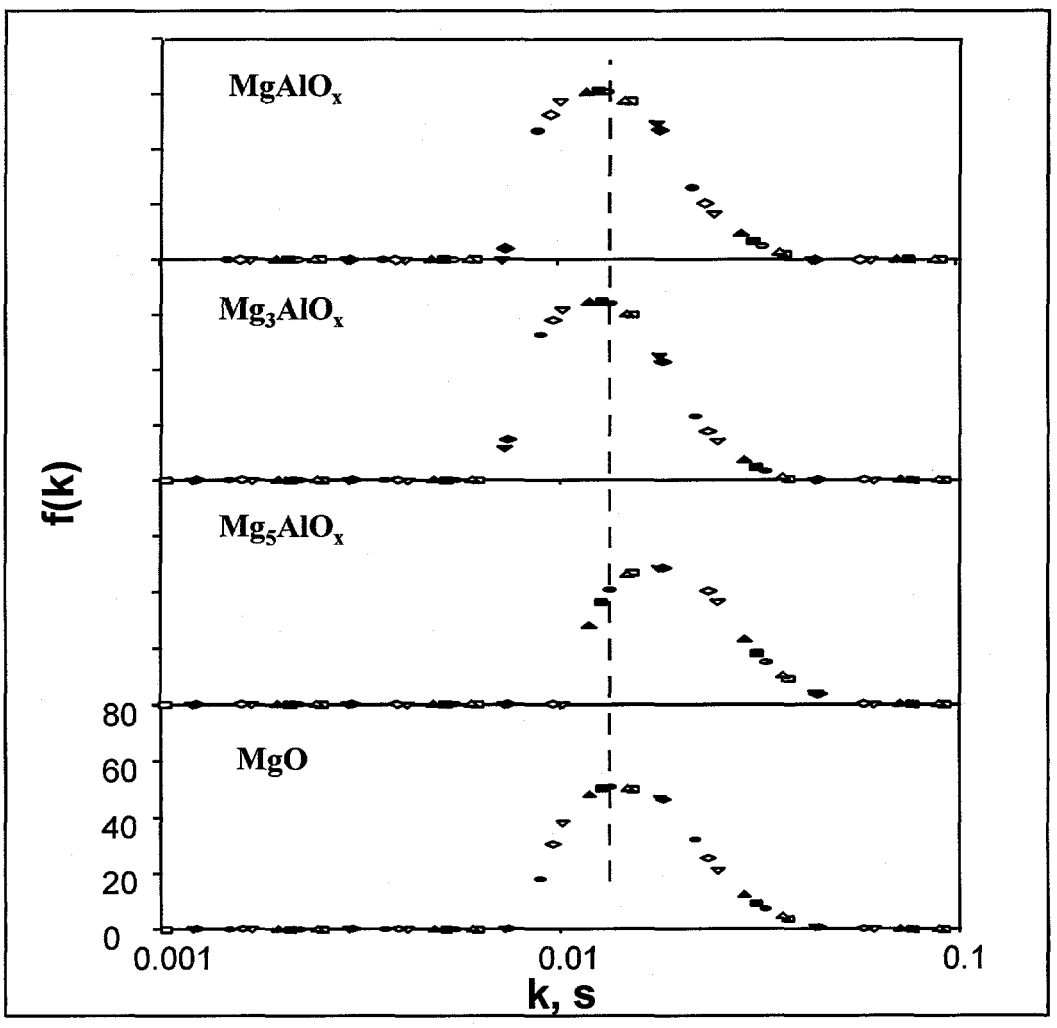

Figure 15. Basic site distribution on pure and Al-modified MgO at 573 K.

The basic site density on MgO determined by the $^{13}CO_2/^{12}CO_2$ exchange method is higher than on any of the $MgAlO_x$ samples (Table 8), suggesting that the addition of Al to MgO decreases the number of basic sites kinetically available at 573 K. The distributions of basic strength among these available basic sites in $MgAlO_x$ and Mg_3AlO_x, however, are comparable to that observed in pure MgO, with exchange rate constants at the maximum distributions of about 1.4×10^{-2} s^{-1} (Figure 15). This suggests that the existence of separate domains of MgO and Al_2O_3 in $MgAlO_x$ and Mg_3AlO_x samples. Only surface MgO contributed to the number of measured basic sites. The basic site density, however, was calculated based on the total surface area (MgO + Al_2O_3). This leads to lower basic site density without any effect on the strength distribution of basic sites related to MgO. Based on the $^{13}CO_2/^{12}CO_2$ isotopic exchange results, one can conclude that MgO and Al_2O_3 exist in separate phase, i.e., no solid solution formed in $MgAlO_x$ and Mg_3AlO_x samples. Both basic site density and strength in Mg_5AlO_x, however, was lower compared to MgO, suggesting the presence of AlO_x decreases the basicity of MgO possibly due to the formation of a Mg-Al-O solid solution.

Task 5: Bench Scale Testing at Air Products and Chemicals

Activities during this reporting period include meeting with Dr. Bernard A. Toseland from Air Products and Chemicals.

Staffing Plans

No changes.

Other activities

Two manuscripts *"Isobutanol and Methanol Synthesis of Copper Catalysts Supported on Modified Magnesium Oxide"* (M. Xu, M.J.L. Gines, B.L. Stephens and E. Iglesia) to be submitted to the Journal of Catalysis and *"Isotopic Switch Methods for the Characterization of Basic Sites in Modified MgO Catalysts"* (M. Xu, M.J.L. Gines and E. Iglesia) to be submitted to the Journal of Physical Chemistry are in the final draft and will be submitted for publication during the next reporting period.

REFERENCES:

1. Apesteguia, C.R., Soled, S.L., Miseo, S., U.S. Patent No. 5,387,570. Issued Feb. 7, 1995 to Exxon Research & Engineering Co., Florham Pk., N.J.
2. Slaa, J.C., van Ommmen, J.G. and J.R.H. Ross, *Catal. Today* **15** (1992) 129.
3. Sofianos, A., *Catal. Today* **15** (1992) 149.
4. Vedage, G.A., Himelfarb, P.B., Simmons, G.W. and K. Klier, *ACS Symp. Ser.* **279** (1985) 295.
5. Elliot, D.J. and F. Penella, *J. Catal.* **119** (1989) 359.
6. Ai, M., *Bull Chem. Japan* **64**(4) (1991) 1342.

7. Ai, M., *J. Catal.* **50** (1977) 291.
8. Luy, J.C., and Parera, J.M., *Appl. Catal.* **26**, 295 (1986).
9. Pines, H., and Manassen, J., *Adv. Catal.* **16**, 49 (1966).
10. Radlowski, C.A., and Hagen, G.P., U.S. Patent No 5,159,125, assigned to Amoco Corporation, Chicago, Ill.
11. Radlowski, C.A., and Hagen, G.P., U.S. Patent No 5,095,156, assigned to Amoco Corporation, Chicago, Ill.
12. King, D.S., and Nix, R.M., *J. Catal.*, **160,** 76 (1996).
13. Iglesia, E. and Boudart, M., *J. Catal.* **81,** 204 (1983).
14. Narita, K., Takeyawa, N., and Toyoshima, I., *React. Kinet. Catal. Lett.* **19,** (1982).
15. Boudart, M., and Djega-Mariadassou, G., "*Kinetics of Heterogeneous Catalytic Reactions*", Princeton Univ. Press, Princeton, N.J. (1984).
16. DePontes, M., Yokomizo, G.H., and Bell, A.T., *J. Catal.* **104,** 147 (1987).
17. McKenzie, A.L., Fishel, C.T., and Davis, R.J., *J. Catal.*, **138**, 547 (1992).
18. Kurokawa, H., Kato, K., Kuwabara, T., Ueda, W., Morikakawa, Y., Moro-Oka, Y., and Ikawa, T., *J. Catal.*, **126**, 208-218 (1990).
19. Pacchioni, G., Ricart, J.M., and Illas, F., *J. Am. Chem. Soc.*, **116**, 10152-8 (1994).
20. Krylov., O.V., "*Catalysis by Nonmetals*", Academic Press, New York and London, 1970).
21. Malinowsky S., Szczepanska S., and Sloczynski, J., *J. Catal.*, **7**, 67 (1967).
22. Choudhary, V.R., Rane, V.H., Catal. Lett., **4**, 101-106 (1990).
23. Reichle, W.T., *J. Catal.*, **94**, 547 (1985).
24. Schaper, H., Berg-Slot, J.J., and Stork,W.H.J., *Appl. Catal*, **54,** 79-90 (1989).
25. Shen, J., Cortright, R.D., Chen, Y., and Dumesic, J.A., *J. Phys. Chem.*, **98**, 8067 (1994).

4. PARTICIPATING PROJECT PERSONNEL

Mingting Xu
Postdoctoral Fellow

Marcelo J. L. Gines
Postdoctoral Fellow

Anne-Mette Hilmen
Postdoctoral Fellow

Zhengjie Hu
Undergraduate Researcher

Bernard A. Toseland
Sub-Contractor
Air Products and Chemicals

Enrique Iglesia
Principal Investigator

DOE F 1332.3
(11-84)

U.S. DEPARTMENT OF ENERGY
MILESTONE SCHEDULE ☐ PLAN ☒ REPORT

FORM APPROVED
OMB 1901-1400

1. TITLE	2. REPORTING PERIOD	3. IDENTIFICATION NUMBER
ISOBUTANOL METHANOL MIXTURE FROM SYNGAS	July 1, 1996-September 30, 1996	DE - AC22 - PC94PC066

4. PARTICIPANT NAME AND ADDRESS	5. START DATE	6. COMPLETION DATE
Department of Chemical Engineering University of California - Berkeley	Oct 1994	Sept 1997

7. ELEMENT CODE	8. REPORTING ELEMENT	9. DURATION	10. PERCENT COMPLETE a Plan	10. PERCENT COMPLETE b Actual
		94 → 95 → 96 → 97 O N D Q2 Q3 Q4 O N D J F M A M J J A S Q1 Q2 Q3 Q4		
	Task 4	Identify reaction intermediates by TPSR and high pressure infrared methods	60	40
	Tasks 3 & 5	Identify catalysts with highest isoalcohol yields (two) and evaluate at conditions resembling envisioned commercial practice.	60	30
	Task 5	Assess economic viability of these catalytic materials	30	0
	Task 5	Complete testing of at least two selected catalysts in slurry reactors.	30	0
	Tasks 3 & 5	Choose two materials for detailed studies of the reaction mechanism and of optimum synthetic protocols	0	0
	Tasks 3 & 5	Complete mechanistic studies on most promising materials	0	0
	Tasks 2 & 5	Develop synthetic procedures that can be carried out on a commercial scale Suggest a range of catalyst compositions for future study.	0	0
	Task 5	Complete testing of the two selected catalytic materials	0	0
	Task 5	Assess future research requirements, technical readiness and economic viability of the most promising approach	0	0
		Produce final report	0	0

DOE F 1332.3
(11-84)

U.S. DEPARTMENT OF ENERGY
MILESTONE SCHEDULE ☐ PLAN ☒ REPORT

FORM APPROVED
OMB 1901-1400

1. TITLE	2. REPORTING PERIOD	3. IDENTIFICATION NUMBER
ISOBUTANOL METHANOL MIXTURE FROM SYNGAS	July 1, 1996 - September 30, 1996	DE - AC22 - PC94PC066

4. PARTICIPANT NAME AND ADDRESS	5. START DATE	6. COMPLETION DATE
Department of Chemical Engineering University of California - Berkeley	Oct 1994	Sept 1997

7. ELEMENT CODE	8. REPORTING ELEMENT	9. DURATION	10. PERCENT COMPLETE a Plan	10. PERCENT COMPLETE b Actual
		94 — 95 — 96 — 97 O N D Q2 Q3 Q4 O N D J F M A M J J A S Q1 Q2 Q3 Q4		
	Task 3	Complete design, construction and start-up of packed bed reactor module	100	100
	Task 2	Prepare Cu-based catalyst compositions and characterize structure, surface area, and effectiveness of several synthetic approaches	100	100
	Task 2	Choose four promising materials for catalyst evaluation	100	100
	Task 3	Construct recirculating reactor module Establish reaction pathways and rate-determining steps	100	100
	Tasks 2 & 3	Identify catalyst components necessary to catalyze rate-determing steps that have been determined	100	100
	Tasks 2 & 3	Identify synthetic techniques to increase the reactivity and accessibility of such required sites	100	100
	Task 4	Complete construction and start-up of temperature programmed surface reaction apparatus and design of high-pressure infrared cell	100	100
	Task 4	Design and construction of high-pressure infrared cell	100	100
	Task 4	Calibrate between UCB and APCI laboratories by testing two selected catalysts in slurry reactors	100	20
	Task 2	Determine the density and reactivity of the required sites and implement synthetic methods to improve them	75	75

1. TITLE	2. REPORTING PERIOD	3. IDENTIFICATION NUMBER
ISOBUTANOL- METHANOL MIXTURE FROM SYNGAS	July 1, 1996 to Set. 30, 1996	DE-AC22-PC94PC066
2. PARTICIPANT NAME AND ADDRESS Department of Chemical Engineering University of California- Berkeley, Berkeley, CA 94720	5. COST PLAN DATE Oct. 15, 1996	6. START DATE OCT 1994 7. COMPLETION DATE OCT 1997

8. Element code	9. Reporting element	ACCRUED COSTS				ESTIMATED ACCRUED COSTS							12. Total contract Value	13. Variance
		Reporting period		Cumulative to date		a.total this fiscal year	b. balance of fiscal year	c. FY96 (1)	d. FY 97 (2)	(3)		e. total		
		a. Actual	b. Plan	c. Actual	d. Plan									
	1. Total (Direct material)	6,870	22,777	75,896	165,152	51,104	40,004	91,109	94,782			210,683	259,929	49,246
	a) Purchased Parts	6,870	9,106	65,995	110,468	42,427	-6,002	36,425	40,200			100,193	98,175	-2,018
	b) Subcontracted Items	0	13,670	3,970	128,722	3,970	50,709	54,679	54,582			109,261	161,754	52,493
	c) Other	0	0	5,931	74,043	4,708	0	0	0			5,931	0	-5,931
	2. Material Overhead	0	0	0	0	0	0	0	0			0	0	0
	3. Direct Labor 'Total	16,662	20,892	110,644	163,921	64,023	19,546	83,569	92,812			223,003	256,725	33,722
	4. Labor Overhead	0	0	0	0	0	0	0	0			0	0	0
	5. Fringe Benefits	1,707	3,350	12,626	26,168	7,300	6,099	13,400	15,368			34,093	41,538	7,445
	6. Special Testing	330	0	2,711	0	1,145	0	0	0			2,711	0	-2,711
	7. Special Equipment	2,168	2,000	290,137	260,000	45,958	-37,958	8,000	0			252,178	260,000	7,822
	8. Travel	1,036	1,629	6,918	12,720	4,731	1,784	6,515	7,020			15,723	19,740	4,017
	9. Consultants	0	0	0	0	0	0	0	0			0	0	0
	10. Other Direct costs	0	6,114	0	47,745	0	24,455	24,455	25,677			50,132	73,422	23,290
	11. Direct costs and Overhead	28,773	56,761	498,932	675,702	174,261	52,783	227,044	235,653			787,368	911,354	123,986
	12. General and Administrative Expense '49.5 %	13,276	20,505	104,077	165,757	64,023	17,997	82,020	90,358			212,431	256,108	43,677
	13. Facilities Capital Cost of Money	0	0	0	0	0	0	0	0			0	0	0
	14. Total Estimated Cost	42,049	77,266	603,009	841,457	238,284	70,778	309,062	326,008			999,795	1,167,462	167,667
	15. Fee	0	0	0	0	0	0	0	0			0	0	0
	16. Cost Sharing	0	9,949	205,766	252,851	17,011	22,786	39,797	56,789			285,341	301,651	16,310
	17. Total estimated DOE funds spent = Item 14-Item 16	42,049	67,316	397,243	588,606	221,273	47,992	269,265	269,219			714,454	865,811	151,357
14. Total		42,049	67,316	397,243	588,606	221,273	47,992	269,265	269,219			714,454	865,811	151,357

15. DOLLARS EXPRESSED IN	16. SIGNATURE OF PARTICIPANT PROJECT MANAGER AND DATE	17. SIGNATURE OF PARTICIPANT'S AUTHORIZED FINANCIAL SERVICE REPRESENTATIVE AND DATE
One U.S. Dollar		Lourdes S. Ferrer